Revista Mexicana de Astronomía y Astrofísica, **51**, 209–219 (2015)

THE NATURE OF THE CM-MM EMISSION IN CLOSE WOLF-RAYET BINARIES

G. Montes,[1,2] A. Alberdi,[2] M. A. Pérez-Torres,[2] and R. F. González [3]

Received September 2 2014; accepted June 5 2015

RESUMEN

El espectro centimétrico de binarias Wolf-Rayet (WR) muestra a menudo la contribución de una región de colisión de vientos (WCR). En sistemas de periodo corto ($\lesssim 1$ año), se espera que este componente sea absorbido por los vientos no chocados, perdiendo el efecto de su condición binaria. Estudios teóricos y observacionales sugieren que en estos sistemas, la WCR puede contribuir a la emisión tanto en la región centimétrica como milimétrica. Analizamos observaciones centimétricas y milimétricas de 17 estrellas WR (incluyendo nueve binarias de periodo corto). Encontramos que para distinguir entre los posibles escenarios son necesarias más observaciones. Enfatizamos la importancia de analizar el espectro utilizando observaciones cuasi-simultáneas en un amplio intervalo de frecuencias para así poder caracterizar y distinguir cualquier posible contribución extra a la emisión.

ABSTRACT

The centimeter spectra of Wolf-Rayet (WR) binaries often show a contribution from a wind-wind collision region (WCR) between the stars. In short period systems ($\lesssim 1$ yr), such a component is expected to be absorbed by the unshocked winds, losing any effect from its binarity. Recent studies suggest that the WCR in these systems may also contribute to the emission at both centimeter and millimeter wavelengths. We analyzed and compared centimeter and millimeter observations of a total sample of 17 WR stars (including nine confirmed short-period systems) to detect any possible WCR contribution. More detailed observations are required in order to distinguish between different scenarios. We highlight the importance of analyzing the spectrum from quasi-simultaneous observations in a wide range of frequencies in order to properly characterize and distinguish any possible extra contribution.

Key Words: binaries: close — radio continuum: stars — stars: winds, outflows — stars: Wolf-Rayet

1. INTRODUCTION

Wolf-Rayet (WR) stars are evolved and massive objects that result from the high mass-loss of O-type stars (Conti 1975). In this stage of evolution, WR stars continue losing material via strong stellar winds with high terminal velocities of $v_\infty \approx 10^3\,\mathrm{km\,s^{-1}}$ and high mass-loss rates of $\dot{M}\approx(10^{-6}$ to $-10^{-5})\,M_\odot\,\mathrm{yr}^{-1}$. The dense and expanding envelope formed by the wind is ionized by the radiation from the central star, resulting in free-free thermal emission detectable from centimeter to millimeter wavelengths (Bieging et al. 1982; Abbott et al. 1986; Leitherer & Robert 1991; Altenhoff et al. 1994; Contreras et al. 1996).

Under the assumptions of a spherically symmetric, isothermal and stationary wind, the flux at radio frequencies has a well characterized spectral index $\alpha \approx 0.6$ ($S_\nu \propto \nu^\alpha$; Panagia & Felli 1975; Wright & Barlow 1975, hereinafter this wind is referred to as standard wind). Observational studies have confirmed such a thermal spectrum for a large sample of WR stars (Abbott et al. 1986; Leitherer et al. 1995, 1997). However, a range of spectral indices

[1]Department of Astronomy and Astrophysics, University of California, Santa Cruz, CA, USA.
[2]Instituto de Astrofísica de Andalucía (IAA), CSIC, Granada, Spain.
[3]Centro de Radioastronomía y Astrofísica, UNAM, México.

have been found with flat ($\alpha \approx 0$), negative and even values higher than the standard 0.6 (Contreras et al. 1996; Chapman et al. 1999; Montes et al. 2009). Such deviations from the thermal spectrum are expected from stellar winds breaking the standard wind assumptions. For instance, changes in the ionization fraction along the emitting regions (Panagia & Felli 1975; Wright & Barlow 1975; Leitherer & Robert 1991), wind structures such as clumps and/or shocks resulting from internal instabilities (e.g. Nugis et al. 1998; González & Cantó 2008) may break the spherical symmetry assumption, resulting in high values for the spectral indices.

Negative and flat spectral indices have been associated with a non-thermal (synchrotron) component of emission arising from a wind-wind collision region (WCR) between the stars in binary systems (typically WR+OB type star; Eichler & Usov 1993). Thus, the detection of a non-thermal spectrum seems to be closely associated with the binary condition of the star. Dougherty & Williams (2000) found that WR binaries with orbital periods $P \gtrsim 1$ yr are usually non-thermal sources, and that those with shorter periods exhibit a thermal spectrum ($\alpha > 0.3$). In the case of short period ($P \lesssim 1$ yr) colliding wind binaries (CWB), the stars are closer and the WCR is likely to lie within the optically thick region of the winds. Thus, in these systems, only the free-free thermal emission from the unshocked winds is thought to be detected, thereby losing any effect from their binarity. However, centimeter observations of WR stars suggest that for some short period systems (e.g. γ^2 Vel, with $P = 78.5$ days, included in this study; Chapman et al. 1999), the non-thermal emission could be able to escape the absorption, contributing to a composite spectrum with a flat spectral index at certain orbital phases.

Theoretical studies suggest that the free-free thermal emission from the WCR may also affect the total radio spectrum, becoming more important as the stars become closer (Stevens 1995; Pittard et al. 2006; Pittard 2010; Montes et al. 2011). The hot material within an adiabatic WCR remains optically thin, contributing with a thermal component of emission with a spectral index of ≈ -0.1 (Pittard et al. 2006) that may dominate the spectrum of the system, particularly at centimeter wavelengths. In this case, the flux density is expected to scale with the binary separation as D^{-1}, becoming more important for closer systems. As the stars get closer, the cooling of the material within the WCR becomes more important, changing from an adiabatic to a radiative WCR (Stevens et al. 1992). In this regime, the emission becomes optically thick, increasing the spectral index to values ≈ 1 (Pittard 2010; Montes et al. 2011); the WCR could also dominate the spectrum, but at millimeter wavelengths, being detectable as an excess of emission with respect to the expected emission from the unshocked winds.

Therefore, even for close WR systems their binarity is likely to affect the resulting radio spectrum for a wide range of frequencies, from centimeter wavelengths (due to a non-thermal and/or an optically thin thermal contribution) to millimeter wavelengths (due to an optically thick contribution detectable as an excess of emission). Hence, in close binaries, it is important to analyze the spectrum by combining observations from centimeter to millimeter wavelengths in order to properly characterize the spectrum and distinguish between all possible contributions. However, at the moment there is a lack of multi-frequency observations of close WR binary systems that would allow a proper determination and analysis of their whole spectra.

In this study, we analyzed the spectrum of a sample of WR stars, collecting observations from centimeter to millimeter wavelengths. The main goal of this work was to detect any possible effect of the WCR over the total spectrum of close WR systems. Thus, we included in our sample both single and binary stars, in order to detect and compare any possible tendency in the spectra of each group of stars. We selected single and close binary stars for which both centimeter and millimeter fluxes were available, making a total sample of 17 WR stars. For two and six stars of the sample, new observations at 20 cm and 1.2 mm are presented, respectively. In § 2, we describe the sample and the new observations reported in this work. The spectral characterizations are described in § 3. Discussion and conclusions are presented in § 4 and § 5, respectively.

2. OBSERVATIONS

We analyzed centimeter and millimeter observations of a total sample of 16 WR stars (see Table 1), from which eight (WR 11, 98, 113, 133, 139, 141, 145, and 156) are confirmed close binaries with orbital periods $P < 1$ year and eight are known as single stars (WR 1, 6, 78, 79a, 105, 110, 135, and 136). We also included the long period system WR 138 for which the influence of its companion over the radio spectrum has not been determined. Centimeter information was taken mainly from the literature (see last column in Table 2 for details), with the exception of the observations performed with the GMRT

TABLE 1

WOLF-RAYET STARS SAMPLE

WR	Spec. Type	Binary Status	P [a]
1	WN4b	S (1)	...
6	WN4	S (2)	...
11	WC8+O9	SB2, VB	78.53
78	WN7h	S	...
79a	WN9ha	(3)	...
98	WN8/WC7	SB1	48.7
105	WN9h	S (2)	...
110	WN5-6	S (4)	...
113	WC8d+O8	SB2	29.7
133	WN5+O9I	SB2, VB	112.4
135	WC8	S	...
136	WN6(h)	S	...
138	WN5+B?	VB(4)	1521
139	WN5+O6V	SB2	4.21
141	WN5+OB	SB2	21.68
145	WN/CE+OB	SB1	20.0
156	WN8h+OB?	d.e.l.	6.5,10,15

[a]Orbital periods for the nine confirmed close binaries are presented in the last column. The values displayed in the columns were taken from the van der Hucht (2001) WR catalog. SB: Spectral Binary; VB: Visual Binary; a: absorption; d.e.l.: diluted emission lines; S: Single. (1): St-Louis (2013); (2): Skinner et al. (2012); (3) Prinja et al. (2001); (4): Chené et al. (2011); (5): Palate et al. (2013).

at 20 cm toward WR 79a and WR 98, and the observations taken from the Very Large Array (VLA) archive for WR 135, 136, 139, and 145 (see Table 2). For the millimeter range, we analyzed observations at 1.2 mm (250 GHz); six of them (for WR 113, 133, 135, 139, 141, and 156) were new reported observations taken with the IRAM 30m telescope. Since flux density and spectral index variability has been reported for some WR stars (specially in binary systems), simultaneous observations are the best way to properly characterize the spectrum of these stars. Thus, in order to minimize the effect of variability on the characterization of the spectrum, we selected observations taken quasi-simultaneously (within the same day), when they were available. Otherwise, we used observations taken on different dates (see Table 2 for details), in order to cover most possible wavelengths.

2.1. *GMRT Observations*

Observations at 1.4 GHz toward WR 79a and WR 98 were performed with the Giant Metrewave Radio Telescope, GMRT[4], during 2007 on four epochs: October 29, November 16, December 8 and December 21. WR 98 was observed in all the epochs, while WR 79a was only observed during November 16. We used the same flux and phase calibrators in all epochs; 3C286 and 1626−298, respectively. Data editing and calibration were carried out using the AIPS package developed by the NRAO. Observations were performed with a bandwidth of 16 MHz covered by 128 channels. The data from five antennas were not taken into account for the calibration. Bandpass calibration was applied using the absolute flux calibrator over 96 central channels.

After a careful editing process, all channels were combined into a single channel. The resulting single channel data were then calibrated following the standard procedure for continuum observations. Self-calibration was applied using the brighter sources present in the field. Finally, we made natural weighting maps for each epoch. In all epochs, we noted strong side-lobes that are probably related to poor uv-coverage. In order to obtain a higher quality map, we stacked the uv data from all observing epochs of WR 98. Finally, we obtained a rms noise of ≈ 0.08 mJy/beam for both WR 98 and WR79a with four hours of time on each source. We did not detect either WR 79a or WR 98, and an upper limit to the flux density of 0.3 mJy (≈ 3 times the rms noise) was determined for both sources.

2.2. *VLA Observations*

We used unreported archival VLA[5] data for WR 135 (1.4, 4.8, 8.4, and 15 GHz), WR 136 (1.4, 4.8, 8.4, and 15 GHz) , WR 139 (4.8 and 8.4 GHz) and WR 145 (4.8 and 8.4 GHz). These observations were performed with the VLA in the A configuration in quasi-simultaneous mode, which allowed us to avoid any effect from a possible variability in flux density. Data editing and calibration were carried out using AIPS, following standard VLA procedures. Off-source rms noises $\approx$ 70μJy, 40 μJy, 30 μJy, 90 μJy, and 100 μJy were obtained at 1.4, 4.8, 8.4, 15, and 23 GHz respectively. We used the AIPS-IMFIT task in order to fit the position and flux

[4]We thank the staff of the GMRT that made these observations possible. GMRT is run by the National Centre for Radio Astrophysics of the Tata Institute of Fundamental Research.

[5]The National Radio Astronomy Observatory is a facility of the National Science Foundation operated under cooperative agreement by Associated Universities, Inc.

TABLE 2

CENTIMETER AND MILLIMETER FLUX DENSITIES

WR	$S_{20\,\mathrm{cm}}$ (mJy)	$S_{6\,\mathrm{cm}}$ (mJy)	$S_{3.6\,\mathrm{cm}}$ (mJy)	$S_{2\,\mathrm{cm}}$ (mJy)	$S_{1.3\,\mathrm{cm}}$ (mJy)	$S_{1.2\,\mathrm{mm}}$ (mJy)	$S_{\mathrm{cm}-1.2\,\mathrm{mm}}$ (mJy)	Obs Date	Ref.
1	...	0.47±0.1	...	...		...		80Jul	(2)
		...	...	...	...	19±5		87Dec	(5)
6	0.57±0.06	1.02±0.05	1.74±0.06	2.38±0.12	3.15±0.22	...	16.3±2.0	99Oct19	(7)
		...	...	...	...	17±3		87Dec	(5)
11			32.50±0.63	67±5		...	467±45	95Jun	(3)
	9.23±0.13	26.50±0.28				...		97Feb	(3)
		...	...	...	...	342±27		90Sep	(4)(9)
78		1.7±0.11	...	2.80±0.22	...	...	9.6±3.0	84Apr04	(1)
		...	...	...	...	11.6±2.3	...	90Sep	(4)
79a	<0.3	0.99±0.05	1.56±0.07	...	2.31±0.16	...	8.9±1.6	08Mar5	(6)
		...	...	...	...	14.7±3.1	...	90Sep	(4)
98	<0.3	0.58±0.06	1.18±0.06	...	1.94±0.16		10.2±2.6	07May06	(6)
		...	...	...	...	19±5		87Dec	(5)
105		2.73±0.11	...	7.63±0.45	...		72.14±16.4	99Nov27	(6)
		...	...	...	...	48±5		87Dec	(4)
110		1.17±0.05	1.77±0.06	2.46±0.12	3.09±0.18	...	13.9±1.9	99Dec26	(8)
		...	...	...	...	32±6		87Dec	(5)
113		0.22±0.03	0.47±0.04	...	1.27±0.08		16.1±3.6	07May06	(6)
		...	...	...	...	4.1±1.1		10Oct28	TS
133		<0.41	0.31±0.03	...	0.57±0.07		2.4±1.2	07May06	(6)
		...	...	...	...	2.6±0.7		10Oct27	TS
135	0.20±0.04	0.42±0.03	0.47±0.08	0.8±0.08	...		4.0±1.26	99Sep	TS
		...	...	...	...	6.7±1.1		10Oct27	TS
136	0.77±0.06	1.87±0.08	2.23±0.07	3.47±0.15	...		19.0±2.2	99Sep	TS
		...	...	...	...	29±3		87Dec	(5)
138		<0.12	0.52±0.03	...	1.15±0.09		7.5±2.2	07May06	(6)
		...	...	...	...	12±4		87Dec	(5)
139		0.26±0.05	0.34±0.04	...	...		1.7±3.2	94Feb	TS
		...	...	...	...	8.5±0.7		10Oct27	TS
141		0.59±0.04	1.28±0.06	...	2.86±0.17		28.5±5.1	08Mar05	(6)
		...	...	...	...	8.0±1.1		10Oct27	TS
145	...	0.77±0.05	1.52±0.05	...	...		87.1±38.9	99Nov	TS
		...	...	...	...	29±7		87Dec	(5)
156		0.77±0.05	0.99±0.05	...	1.59±0.10		4.8±0.9	08Mar05	(6)
		...	...	...	...	8.9±1.0		10Oct27	TS

Columns 2 to 7 show the flux densities obtained from observations. Column 8 ($S_{\mathrm{cm}-1.2\,\mathrm{mm}}$) shows millimeter flux densities obtained from the extrapolation of the centimeter spectrum to 1.2 mm. The last column shows the references from the centimeter and millimeter wavelengths of each star. The upper limits at 20 cm for WR 79a and WR 98 were obtained from observations performed between Oct-Dec, 2007. (1): Abbott et al. (1986); (2): Bieging et al. (1982); (3): Chapman et al. (1999) ; (4): Leitherer & Robert (1991); (5): Altenhoff et al. (1994); (6): Montes et al. (2009); (7): Skinner et al. (2002a); (8): Skinner et al. (2002b); (9): Williams et al. (1990); TS: This Study.

density of the detected sources. Since the sources were consistent with an unresolved structure, as expected, we fixed the standard parameters for point-like sources in IMFIT. Flux densities and their uncertainties are shown in Table 2.

2.3. *IRAM 30m telescope Observations*

We performed observations with the IRAM[6] 30m telescope located in Pico Veleta (Sierra Nevada, Spain) using the bolometer camera MAMBO2 in the ON-OFF mode. This camera operates at 250 GHz (1.2 mm wavelength) with a HPBW (half power beam width) of 11". The six WR stars were observed during the pool observing session in October/November of 2010. To minimize the effect of atmospheric absorption, the science targets were observed at elevations $\geq 45°$. The ON-OFF observations were centered on the most sensitive pixel, number 20. Each source was typically observed in several blocks of 20 minute integrations. Throughout the observing runs, gain calibration was performed by observing Neptune, Uranus or Mars. Total power measurements at different elevations were made to infer the atmospheric opacity (skydip).

The data were reduced using the MOPSIC pipeline (developed by R. Zylka). We reached an rms of $\approx 1\,\mathrm{mJy\,beam^{-1}}$ and $\approx 0.7\,\mathrm{mJy\,beam^{-1}}$ with 20 and 60 minutes of integration, respectively. The forward efficiency (Feff) was found to be not stable during the whole pool observing session. We tested the stability of our observations by calibrating the sub-scan separately for those sources for which more than one scan was taken and did not detect any significant effect on our rms noise and flux density determinations. We detected the six observed sources; the flux densities obtained are presented in Table 2.

3. RADIO SPECTRAL CLASSIFICATION

In this Section we classified the spectra of the WR stars in our sample by comparing the centimeter and the millimeter spectral indices. Spectral indices at each wavelength range were determined from the flux densities presented in Table 2.

Note that for binary stars, the orbital motion may produce variability due to changes in the absorption from the unshocked winds and/or to changes in the separation of the stars in eccentric systems (see for instance Pittard 2010). Thus, as we pointed out in § 2, the best way to determine the spectrum for these stars is through the analysis of multi-wavelength observations taken quasi-simultaneously at all the observed wavelengths. However, these observations, covering from centimeter to millimeter wavelengths, are difficult to make, since covering both wavelength ranges usually requires different instruments, which makes the observations difficult to schedule under the simultaneity requirement. Here, we try to minimize the variability effect, at least at centimeter wavelengths, by selecting simultaneous observations when they were available (see Columns 9 and 10 in Table 2 for observation date details). Furthermore, WR single stars also show variability in their stellar winds that may result from internal structures which mainly affect the UV and visible spectra (St-Louis 2013). Such structures are not expected to be relevant in the large scale regions where the radio emission comes from.

Expected flux densities at 1.2 mm were calculated by extrapolating the centimeter spectrum, which was characterized by determining a centimeter spectral index, $\alpha_{\rm cm}$. The spectral indices were calculated using a linear regression fit, weighting each flux point by its error, or using the logarithmic ratio of the flux densities and the frequencies when only two frequencies were available. In the case of the sources for which more than one set of observations were reported, we characterized the centimeter spectrum using only the fluxes at the epoch when the spectrum was classified as thermal based on the shorter wavelengths. In this "thermal" state, any possible contribution from a WCR at the centimeter range would be minimum. This allowed us to identify any possible change in the spectrum at the millimeter range. Furthermore, centimeter-millimeter spectral indices, $\alpha_{\rm cm-mm}$, were determined using the flux density at 1.2 mm and that at the shorter wavelength from the centimeter observations (Table 2).

Thus, we compared the fluxes at 1.2 mm obtained from the extrapolation with those obtained from observations. From this comparison, we considered that there was an excess or deficit in the flux density at 1.2 mm when the measured and the extrapolated values did not agree within two times their uncertainties. The difference between these two values implied a change in the spectrum behavior from the centimeter to the millimeter range, which was also shown by the difference (marginal, in most of the cases) between $\alpha_{\rm cm}$ and $\alpha_{\rm cm-mm}$ in Table 3. However, the lack of observations at intermediate

[6]We thank the staff of IRAM for help providing during the observations. IRAM is supported by INSU/CNRS (France), MPG (Germany) and IGN (Spain).

TABLE 3

SPECTRAL INDICES

WR	$\alpha_{\rm cm}$	$\alpha_{\rm cm-mm}$
1	...	0.9±0.2
6	0.67±0.04	0.7±0.2
11	0.74±0.02	0.6±0.1
78	0.44±0.21	0.50±0.2
79a	0.54±0.05	0.8±0.2
98	0.65±0.08	1.0±0.3
105	0.83±0.15	0.68±0.1
110	0.62±0.04	1.0±0.2
113	1.06±0.08	0.5±0.3
133	0.60±0.37	0.6±0.3
135	0.58±0.09	0.8±0.2
136	0.61±0.03	0.8±0.1
138	0.79±0.23	1.0±0.3
139	0.47±0.93	0.9±0.1
141	0.94±0.06	0.4±0.1
145	1.19±0.28	0.9±0.2
156	0.46±0.06	0.7±0.1

wavelengths did not allow to properly determine the spectral index and made any changes in spectrum less evident.

In Figures 1 (single) and 2 (binaries) we plotted the flux measurements and the extrapolation of centimeter fluxes and of the measurements between centimeter to millimeter fluxes. According to our criteria, we found that most of the sources (12 in a sample of 16) showed a millimeter flux that was in agreement with the prediction from the centimeter fluxes. We also found two stars (WR 110 and 156) showing an excess of emission at millimeter wavelengths compared to the value obtained from the extrapolation of the centimeter spectrum (see their corresponding panels in Figures 1 and 2). The $\alpha_{\rm cm-mm}$ values of these sources also suggested an increase of the spectral index towards millimeter wavelengths. Finally, for WR 113 and WR 141 the flux density at millimeter wavelengths was below the value obtained from the extrapolation of centimeter observations. The radio spectra of these stars also showed a change in the slope (see Figure 2), with spectral indices changing from values higher than 0.6 at centimeter wavelengths, to values similar to the 0.6 expected for a standard wind at millimeter wavelengths. In the following section, we discuss possible scenarios that could explain the different spectra found.

4. DISCUSSION

Deviations in the wind parameters from those assumed by the standard wind model may change the resulting spectral index (see e.g. Wright & Barlow 1975; Panagia & Felli 1975). In binary systems, the contribution of an extra component of emission such as a WCR between the stars may also change the radio spectrum. This effect has been explored mainly for wide systems, where the WCR lies outside the central optically thick region. The emission from the WCR was then able to avoid the free-free absorption from the unshocked winds, contributing a non-thermal component of emission and resulting in a flat (or even negative) spectral index at centimeter wavelengths (e.g. WR 146 and WR 147; Dougherty et al. 2000; Williams et al. 1997). However, in the case of close systems, although theoretical studies suggest that the presence of a binary companion may also impact the total radio spectrum (Stevens 1995; Pittard 2010; Montes et al. 2011), these results remain observationally unexplored.

In general, the nature of stellar winds from WR stars remains poorly understood. For instance, the acceleration process seems to be subject to instabilities that deviate the wind from being the smooth, steady outflow assumed by the standard wind model. Evidences of such deviations are seen along different ranges of the electromagnetic spectrum, from the stellar rotation changing the shapes of the emission lines in the *UV* (e.g. Hamann et al. 2006), to the heat shocked structures emitting at X-ray wavelengths (Skinner et al. 2012). Dust formation has been detected for several WC type stars (Williams 2014). The high densities reached in the WCR allow the formation of dust despite the high radiation from the stars. With temperatures $\gtrsim$ 800 K, the emission becomes detectable at wavelenghts shorter than IR (e.g. WR 104; Williams 2008; Tuthill et al. 2008) and no contribution is expected at radio or millimeter ranges. At radio wavelengths, the emission arises from the external regions of the wind (10^{14} cm at 6 cm; 5 GHz), and the effect from the innermost structures in the wind is expected to be diminished at such large distances from the star. This seems to be supported by our results from the spectral characterization of the stars in the sample, where 12 of the 16 stars showed a radio spectrum which was roughly in agreement with that expected for a standard wind.

The dependence of structure, ionization state, and/or velocity of the wind on the distance from the star is expected to affect the radio spectrum (e.g. Wright & Barlow 1975; Leitherer & Robert 1991). The characteristic size of the radio emitting region

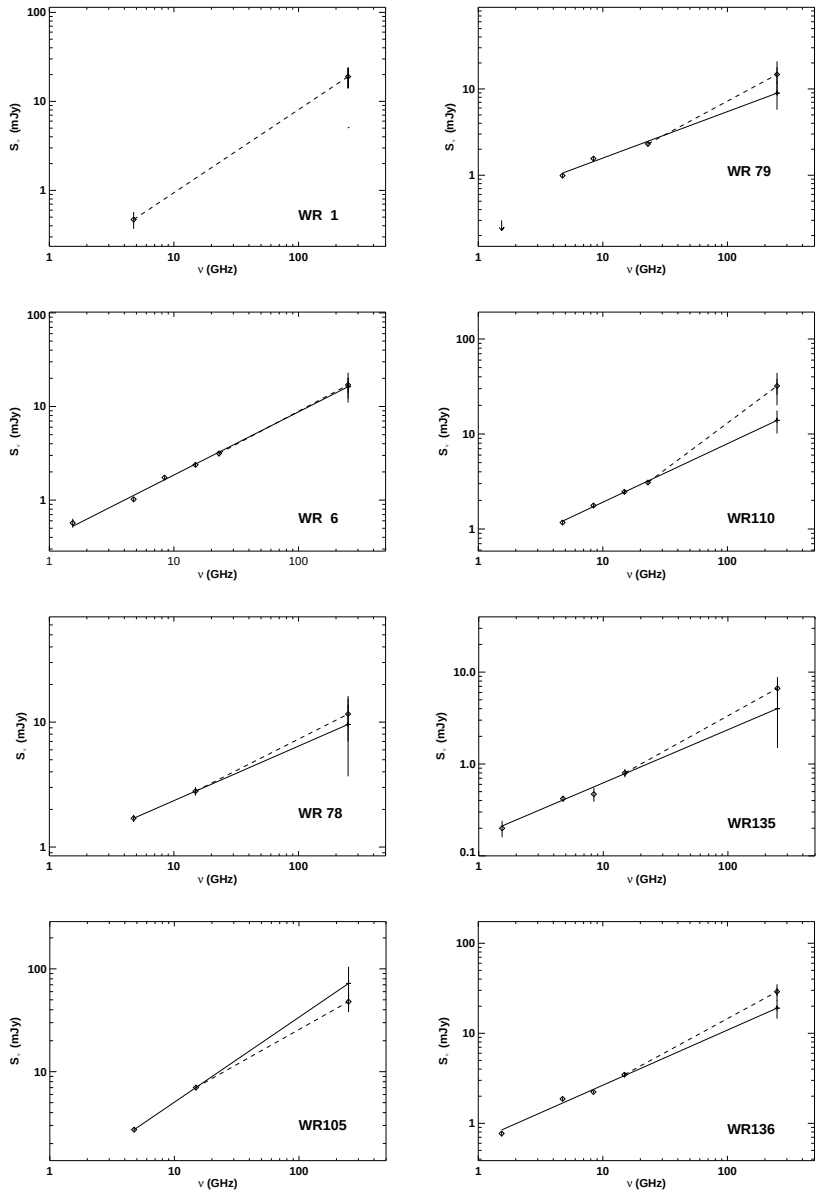

Fig. 1. Extrapolation of the centimeter spectrum to millimeter wavelengths (solid line) and comparison with the millimeter spectrum determined from observations (dashed line) for the *single* stars of the sample. The filled circles represent the observed flux densities. Note that, according to our criteria, WR 110 shows an increase of the spectrum towards short wavelengths.

increases as a power-law (~ 0.7) with wavelength (Wright & Barlow 1975; Panagia & Felli 1975); the typical sizes are $\approx 10^{14}$ cm and $\approx 10^{13}$ cm for the centimeter and millimeter ranges, respectively. It was thus expected that the instabilities and inhomogeneities, present mainly in the inner regions of the wind, would have a stronger effect at millimeter than at centimeter wavelenghts, resulting in a steepening of the spectrum (towards short wavelengths; Nugis et al. 1998, Blomme 2011), similar to that observed for WR 110 and WR 156.

For WR 113 and WR 141, the deficit in the millimeter flux with respect to the extrapolated value obtained from the centimeter observations implied a change in the spectrum from a steep ($\alpha \approx 1$) behavior at centimeter wavelengths to a standard behavior ($\alpha \approx 0.6$) at millimeter ones. We did not find this kind of spectrum in any of the single stars in

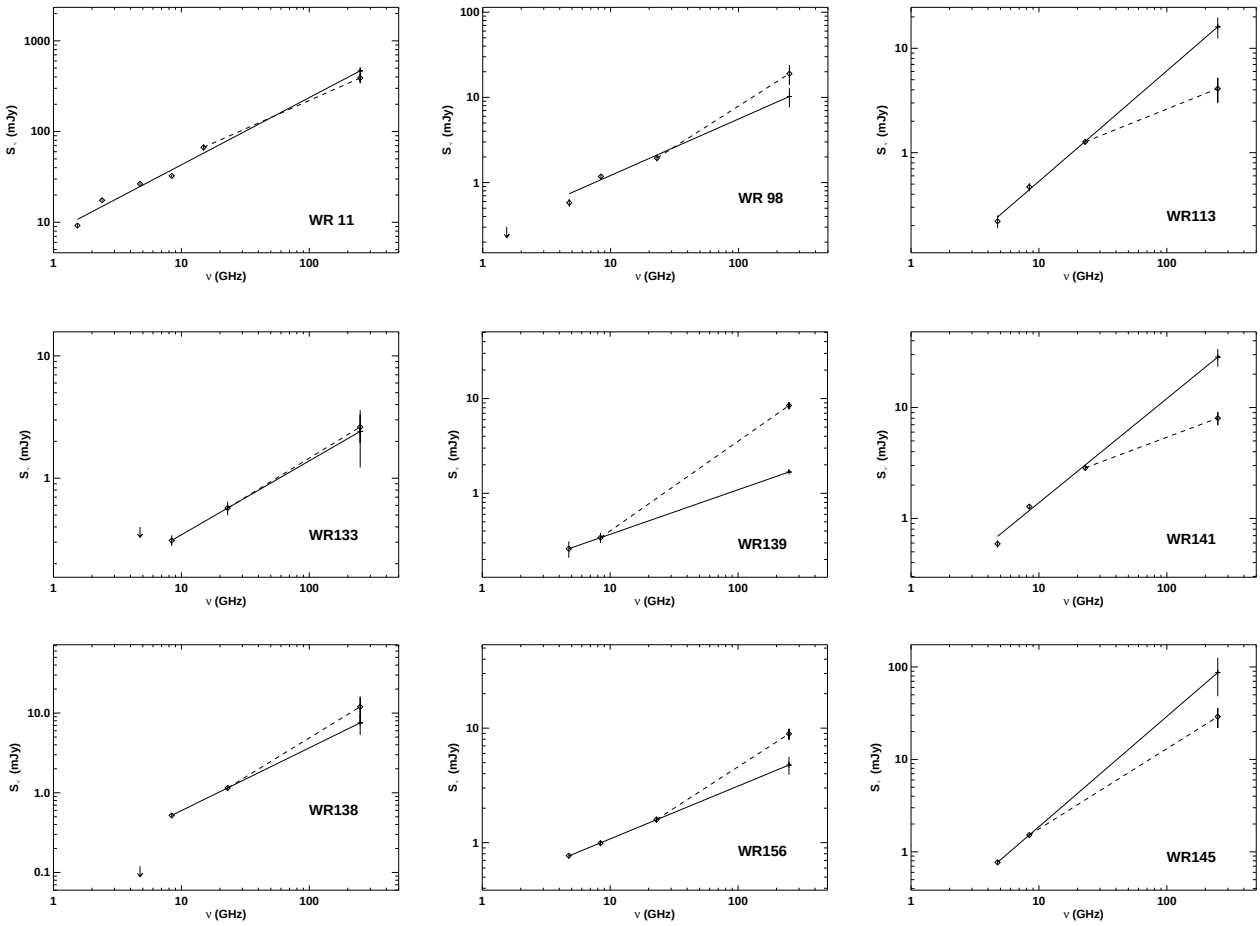

Fig. 2. Extrapolation of the centimeter spectrum to millimeter wavelengths (solid line) and comparison with the millimeter spectrum determined from observations (dashed line) for the *binary* stars. The filled circles represent the observed flux densities. Note that, according to our criteria, the spectrum of WR 113 and WR 141 show a "deficit" in the emission at millimeter, and the spectrum of WR 156 indicate a steepening toward short wavelengths.

our sample, suggesting that it could be related to a binary scenario. Indeed, such a steep spectrum at centimeter wavelenghts is difficult to explain in a single thermal stellar wind context, since it would imply that the emission at these wavelengths is dominated by an optically thick region. However, such an optically thick region would be very near the star and would have a small size, of the order of 10^{14} cm for a typical WR wind, which at a distance of $\approx$1 kpc (the typical distance for the stars in the sample, see Table 1) would have an angular size of only a few milliarcseconds. Since the angular resolutions at centimeter wavelengths for WR 113 and WR 141 observations are of the order of arcsecs, we were actually capturing emission from an extended and optically-thin region, for which lower value for the spectral index was expected. Another possible explanation for the deficit in the millimeter emission of these stars may be that an extra contribution of a non-thermal component (or optically-thin thermal emission with $\alpha \approx -0.1$; see Pittard et al. 2006) is highly affected by the free-free absorption from the unshocked winds. For close systems, absorption effects become more important, since the WCR lies closer to the stars and is surrounded by the denser regions on the wind. The free-free absorption from the unshocked winds will mainly affect the emission at longer wavelengths (with the free-free absorption coefficient $\alpha_\lambda \sim \lambda^2$) resulting in a steepening of the spectrum in this range. Furthermore, at short wavelengths, the non-thermal emission could also be diminished by inverse Compton cooling, which is likely to be important in such close binary systems (see Pittard et al. 2006). Thus, for WR 113 and WR 141,

a possible WCR contribution would be more relevant at intermediate wavelengths, with a spectrum dominated by thermal emission at the longest and shortest wavelengths.

We investigated whether a WCR component of emission could actually be able to escape the free-free absorption in the case of WR 113 and WR 141, by calculating the P_{cr}, which is defined as a critical period over which the emission at a frequency ν from a WCR could be able to escape the absorption (equation 22 in Eichler & Usov 1993). We estimated P_{cr} at the intermediate frequency of ν =23 GHz (1.3 cm) and assumed the following: WR wind parameters, $\dot{M} = 2 \times 10^{-5}\, M_{\odot}\,\mathrm{yr}^{-1}$ and $v = 1700\,\mathrm{km\,s}^{-1}$ (Lamontagne et al. 1996) for WR 113, and $\dot{M} = 2.6 \times 10^{-5}\, M_{\odot}\,\mathrm{yr}^{-1}$ and $v = 1550\,\mathrm{km\,s}^{-1}$ (Montes et al. 2009; Eenens & Williams 1994) for WR 141. Regarding the wind momentum ratio of the WR star and the O star companion (typical value for WR+O type systems) we assumed the value of ≈ 0.1. In the case of WR 113, we found $P_{crit} \approx 17$ days, which was smaller than the orbital period, $P \approx 29.7$ days. Furthermore, for WR 141, we obtained $P_{crit} \approx 20$ days, which was similar to its orbital period $P \approx 21.6$ days. Thus, at least for WR113 (and marginally for WR 141), the non-thermal emission from the WCR could be able to escape the absorption, at least at certain orbital phases.

For WR 98, there were previous reports of variability at 6 cm, which converted the spectral index ($\alpha_{6-3.6\,\mathrm{cm}}$) from a standard to a flat value (≈ 0.3) (Montes et al. 2009). The short variability timescale of $\approx$15 days, about a third of its orbital period ($P \approx 48.7$ days), suggested that it could be related to the orbital motion of the stars. Flux density variability is often observed in CWB, suggesting the presence of an extra component of emission arising from the WCR (e.g. WR 140; Dougherty et al. 2005). However, for short period binaries, variability has not been proven to be related to a binary scenario, and more observations covering a complete orbit are required in order to corroborate this for WR 98. The variability in WR 98a might be an indication of a non-thermal component being absorbed at certain orbital phases, which is also supported by the low values of the upper limits of the fluxes at 20 cm (see Table 3). Furthermore, the spectral indices of WR 98 suggest (although marginally) a steepening of the spectrum towards short wavelenghts (see Table 3). Such behavior is expected for short period systems where a highly radiative shock structure may be able to contribute with an optically-thick component of thermal emission (with a spectral index ≈ 1 Pittard 2010; Montes et al. 2011). Millimeter observations with lower flux uncertainties are required in order to corroborate such emitting component in WR 98.

Finally, for WR 79a and WR 105, the spectral indices and variability from previous observations at centimeter wavelengths indicate that non-thermal emission could be contributing to the spectrum (Montes et al. 2009). The high value of the $\alpha_{\mathrm{cm}} \approx 0.83$ of WR 105 suggests that a non-thermal absorbed component may be present in the "thermal" state. The origin of a non-thermal spectrum in single stars remains unclear. A study of the non-thermal emission produced by wind-embedded shocks within a single O-type stellar wind found that the radial decline of the shock strength (velocity jump and compression ratio) produces a rapid decrease of the synchrotron emission, which becomes negligible at those radii where the stellar wind becomes optically thin (van Loo et al. 2006). This rules out the detection of a non-thermal spectrum for single stars. Moreover, as pointed out by Dougherty & Williams (2000), proving that a star is single is very difficult, and we cannot rule out the presence of a companion in these stars.

5. CONCLUSIONS

The effect of binarity in wide systems results mainly from the contribution of non-thermal emission at centimeter wavelengths. However, theoretical work suggest that close binaries present a more complex scenario, where the WCR may contribute at very different wavelength ranges, depending on the nature of the shocks, which can be either adiabatic or radiative. This may have a high influence on the final spectrum, and hence on the nature of the resulting emission, which can be non-thermal and/or (optically-thin or thick) thermal emission. Therefore, we highlight the importance of monitoring the spectrum of WR stars based on quasi-simultaneous observations in a wide range of wavelengths at different positions along the orbital period in order to properly characterize the spectrum and distinguish between all possible contributions. From our analysis of the centimeter to millimeter observations of WR stars, we found hints of a WCR contribution for WR 98, WR113, and WR141. However, the available observations did not allow us to distinguish between the different scenarios that could result in a similar spectrum.

The new generation of ultra-sensitive instruments operating at centimeter (e.g., JVLA, ATCA), millimeter, and submillimeter wavelengths (e.g.,

CARMA, ALMA) offer the opportunity to improve and to extend the observations to shorter frequencies in order to perform this kind of studies with more detail. In the case of wide binary systems, high angular resolution has allowed to spatially resolve the non-thermal emission from the WCR, leading to an unequivocal identification of a contribution of WCR emission. However, in the case of close WR stars, the emission is unlikely to be spatially resolved even with the new powerful instrumentation, since the WCR should be very near to the unshocked stellar wind region, and an angular resolution of less than 0.05 mas would be required for a binary with an orbital period of ≈ 1 year and a total mass of $\approx 50\ M_{\odot}$ at a distance of 1 kpc (the highest angular resolution, obtained with VLBI techniques, is ≈ 1 mas Dougherty et al. 2005; Ortiz-León et al. 2011). Nevertheless, since the thermal component of emission from the WCR is expected to be modulated by the orbital motion, with a strong dependence on the inclination angle of the orbit, a way to determine a thermal WCR contribution for WR113, WR141, and WR156, could be through the relation between variability and orbital period, by sampling a light curve along a complete period, at least at one frequency.

G.M. acknowledges financial support from the CSIC JAE-PREDOC and AAUW Postdoctoral Fellowships, as well as Carlos E. Carrasco-González for a critical reading of this paper. This research was partially supported by the Spanish MICINN through grant AYA2009-13036-CO2-01, cofunded with FEDER funds. RFG acknowledges support from Grant PAPIIT IN100511 and PAPIIT IN112014, UNAM, México.

REFERENCES

Abbott, D. C., Beiging, J. H., Churchwell, E., & Torres, A. V. 1986, ApJ, 303, 239
Altenhoff, W. J., Thum, C., & Wendker, H. J. 1994, A&A, 281, 161
Bieging, J. H., Abbott, D. C., & Churchwell, E. B. 1982, ApJ, 263, 207
Blomme, R. 2011, Bulletin de la Societe Royale des Sciences de Liege, 80, 67
Chapman, J. M., Leitherer, C., Koribalski, B., Bouter, R., & Storey, M. 1999, ApJ, 518, 890
Chené, A.-N., Moffat, A. F. J., Cameron, C., et al. 2011, ApJ, 735, 34
Conti, P. S. 1975, Memoires of the Societe Royale des Sciences de Liege, 9, 193
Contreras, M. E., Rodríguez, L. F., Gómez, Y., & Velázquez, A. 1996, ApJ, 469, 329
Dougherty, S. M., & Williams, P. M. 2000, MNRAS, 319, 1005
Dougherty, S. M., Williams, P. M., & Pollacco, D. L. 2000, MNRAS, 316, 143
Dougherty, S. M., Beasley, A. J., Claussen, M. J., Zauderer, B. A., & Bolingbroke, N. J. 2005, ApJ, 623, 447
Eenens, P. R. J., & Williams, P. M. 1994, MNRAS, 269, 1082
Eichler, D., & Usov, V. 1993, ApJ, 402, 271
González, R. F., & Cantó, J. 2008, A&A, 477, 373
Hamann, W.-R., Gräfener, G., & Liermann, A. 2006, A&A, 457, 1015
Lamontagne, R., Moffat, A. F. J., Drissen, L., Robert, C., & Matthews, J. M. 1996, AJ, 112, 2227
Leitherer, C., & Robert, C. 1991, ApJ, 377, 629
Leitherer, C., Chapman, J. M., & Koribalski, B. 1995, ApJ, 450, 289
Leitherer, C., Chapman, J. M., & Koribalski, B. 1997, ApJ, 481, 898
Montes, G., Pérez-Torres, M. A., Alberdi, A., & González, R. F. 2009, ApJ, 705, 899
Montes, G., González, R. F., Cantó, J., Pérez-Torres, M. A., & Alberdi, A. 2011, A&A, 531, A52
Nugis, T., Crowther, P. A., & Willis, A. J. 1998, A&A, 333, 956
Ortiz-León, G. N., Loinard, L., Rodríguez, L. F., Mioduszewski, A. J., & Dzib, S. A. 2011, ApJ, 737, 30
Palate, M., Rauw, G., De Becker, M., Nazé, Y., & Eenens, P. 2013, A&A, 560, AA27
Panagia, N., & Felli, M. 1975, A&A, 39, 1
Pittard, J. M., Dougherty, S. M., Coker, R. F., O'Connor, E., & Bolingbroke, N. J. 2006, A&A, 446, 1001
Pittard, J. M. 2010, MNRAS, 403, 1633
Prinja, R. K., Stahl, O., Kaufer, A., et al. 2001, A&A, 367, 891
Skinner, S. L., Zhekov, S. A., Güdel, M., & Schmutz, W. 2002a, ApJ, 579, 764
Skinner, S. L., Zhekov, S. A., Güdel, M., & Schmutz, W. 2002b, ApJ, 572, 477
Skinner, S. L., Zhekov, S. A., Güdel, M., Schmutz, W., & Sokal, K. R. 2012, AJ, 143, 116
St-Louis, N. 2013, ApJ, 777, 9
Stevens, I. R., Blondin, J. M., & Pollock, A. M. T. 1992, ApJ, 386, 265
Stevens, I. R. 1995, MNRAS, 277, 163
Tuthill, P. G., Monnier, J. D., Lawrance, N., et al. 2008, ApJ, 675, 698
van der Hucht, K. A. 2001, NAR, 45, 135
van Loo, S., Runacres, M. C., & Blomme, R. 2006, A&A, 452, 1011
Williams, P. M., van der Hucht, K. A., Sandell, G., & The, P. S. 1990, MNRAS, 244, 101
Williams, P. M., Dougherty, S. M., Davis, R. J., et al. 1997, MNRAS, 289, 10
Williams, P. M. 2008, RMxAC, 33, 71
Williams, P. M. 2014, MNRAS, 445, 1253
Wright, A. E., & Barlow, M. J. 1975, MNRAS, 170, 41

A. Alberdi and M. A. Pérez-Torres: Instituto de Astrofísica de Andalucía (IAA), CSIC, Glorieta de la Astronomía s/n, E-18008, Granada, Spain.
R. F. González: Centro de Radioastronomía y Astrofísica, UNAM, México.
Gabriela Montes: Department of Astronomy and Astrophysics, University of California, Santa Cruz, CA 95064 (gmontes@ucsc.edu).